

due to disparate cues and domain gaps [2].

In this work, we propose a *Paired-Sampling Contrastive* framework that unifies PAD and DFD under a single-model architecture. Our key idea presented on Fig. 1 is to form matched pairs of genuine and attack face embeddings, and to apply *asymmetric augmentations* only to the genuine samples. A ConvNeXt-v2-Tiny backbone then optimizes both a binary classification loss (to separate live vs. attack) and a supervised contrastive loss (to pull genuine features together and push all attack features apart), while CutMix regularization simulates partial occlusions and encourages the network to rely on distributed liveness cues. Challenge results demonstrate that our approach achieves an average classification error rate (ACER) of 2.10%, ranking among the top-performing solutions.

2. Related work

Image-based physical presentation attacks and digital forgeries detection approaches analyze single images to identify spoofing without relying on temporal cues. Recent advancements span diverse model architectures, generalization strategies, and benchmark datasets.

Model Architectures. CNN-based methods, particularly EfficientNets [3], have been popular due to their strong feature extraction capabilities and robustness to subtle visual artifacts [4]. However, CNN models often face limitations in generalizing beyond training datasets. Vision Transformers (ViTs) [5] have recently emerged as effective alternatives, leveraging long-range dependencies within images to detect manipulation inconsistencies. For instance, Luo et al. introduced adaptive modules on pre-trained ViTs, significantly enhancing cross-dataset detection accuracy [6]. Multi-task models like LAA-Net combine CNN backbones with attention mechanisms, explicitly focusing on localized blending artifacts to identify high-quality deepfakes [7]. Additionally, hybrid frameworks such as TruFor fuse visual features with noise residuals through transformer architectures, improving detection across diverse forgery types [8].

Generalization Strategies. A core challenge remains the generalization across different deepfake datasets. Data augmentation techniques like compression, blurring, and color adjustments effectively enhance model robustness [9]. In [10], the authors demonstrated improved generalization by generating synthetic data through blending real faces, creating forgery-like artifacts without deepfake-specific models. Identity-invariant learning also plays a crucial role by reducing implicit identity bias, ensuring models focus on manipulation artifacts rather than specific facial identities [11].

Datasets. Standardized benchmarks drive the evaluation of detection methods. FaceForensics++ is widely utilized for initial training, but its limitations necessitate test-

ing on more challenging sets like Celeb-DF and DFDC to assess generalization capabilities [12–14]. Other datasets such as WildDeepfake offer real-world complexities that further challenge models to generalize effectively beyond controlled scenarios [15].

Joint Physical and Digital Attack Datasets. Emerging threats have expanded the scope of deepfake detection research to simultaneously address both digital manipulations and physical presentation attacks (PAD). These combined datasets integrate diverse attack vectors, providing richer benchmarks that test detectors’ robustness across various attack modalities. GrandFake [16] merges PAD and digital deepfake datasets, encompassing a broad spectrum of 25 distinct attack types. This comprehensive dataset aids in developing unified detection methods capable of identifying diverse forgery and spoofing attempts simultaneously. Similarly, in [2], nine different PAD and forgery datasets were consolidated, emphasizing the critical issue of identity confounders. It facilitates the analysis of detectors’ vulnerability to identity-specific biases and supports strategies aimed at creating identity-invariant detection models. UniAttackData [1] presents a notable advancement by maintaining identity consistency across both physical and digital attacks for each subject. This design uniquely enables models to learn consistent identity-based features, thus enhancing generalization and robustness across various types of manipulations.

In summary, image-based physical presentation attacks and digital forgeries detection methods have evolved significantly through the integration of advanced architectures and generalization strategies. Continued progress relies on combining these innovations to maintain robustness against increasingly sophisticated forgeries.

3. Methodology

In this section we outline the three core components of the proposed approach. Sec. 3.1 introduces our data filtering pipeline. Subsequently, Sec. 3.2 contains details of the paired setup employed during training. Finally, Sec. 3.3 explains the contrastive training procedure used for representation learning.

3.1. Data filtering

During manual analysis of the training dataset, we encountered a significant number of live samples that did not contain faces or any valuable information. To ensure the training setup includes only valid live samples, we manually filtered the live subset, removing approximately 10% of non-valid images from the original set.

To eliminate potential bias from identities that appear only in the spoofing subset, we propose a filtering pipeline based on a face recognition system. First, we extract 512-dimensional face embeddings for all training images using a

pretrained InceptionResNet-v1 model [17]. In parallel, we obtain face bounding boxes with the MTCNN detector [18].

Next, we compute the cosine similarity between each spoofing attack sample and all live samples available in the training data:

$$\text{sim}(a, b) = \frac{\langle a, b \rangle}{\|a\|_2 \|b\|_2},$$

where $a, b \in \mathbb{R}^{512}$ are the InceptionResNet-v1 face embeddings of a spoof-attack image and a live image, respectively.

For each spoofing attack sample we find live sample with the highest similarity:

$$b^*(a) = \arg \max_{l \in \mathcal{L}} \text{sim}(a, l),$$

with \mathcal{L} denoting all live embeddings in the training set.

To proceed with filtering, we keep a spoofing attack sample only if its similarity to the most similar live sample exceeds a predefined threshold:

$$\mathcal{D}_{\text{train}} = \{ (a, b^*(a)) \mid a \in \mathcal{A}, \text{sim}(a, b^*(a)) > \tau_{\text{sim}} \},$$

where \mathcal{A} is the set of all attack embeddings and τ_{sim} is the cosine-similarity threshold. We treat similarity as a training hyperparameter that can be optimized based on the target metric on the validation subset.

As a result of the filtering procedure (Tab. 1), certain types of presentation attacks were entirely removed from the training set due to the lack of sufficiently similar live counterparts. In particular, all PAD attacks such as Replay, Print, and Cutouts were completely filtered out. Furthermore, digital attack types such as Face Swap and Attribute Edit were almost entirely eliminated, with only a small fraction of samples remaining after similarity-based filtering.

Category	Before Filtering	After Filtering
Pixel-Level	8 364	5 024
Semantic-Level	3 757	2 349
Video-Driven	1 540	520
Face-Swap	6 160	20
Attribute-Edit	1 476	5
Replay	109	–
Cutouts	79	–
Print	43	–
Live Face	839	751

Table 1. Sample distribution across attack categories in train subset before and after proposed filtering.

3.2. Sampling setup

Motivated by the large number of pixel-level, adversarial, and attribute-editing attacks that preserve the original identity while introducing subtle manipulations, we aim to improve model sensitivity to these fine-grained artifacts. To

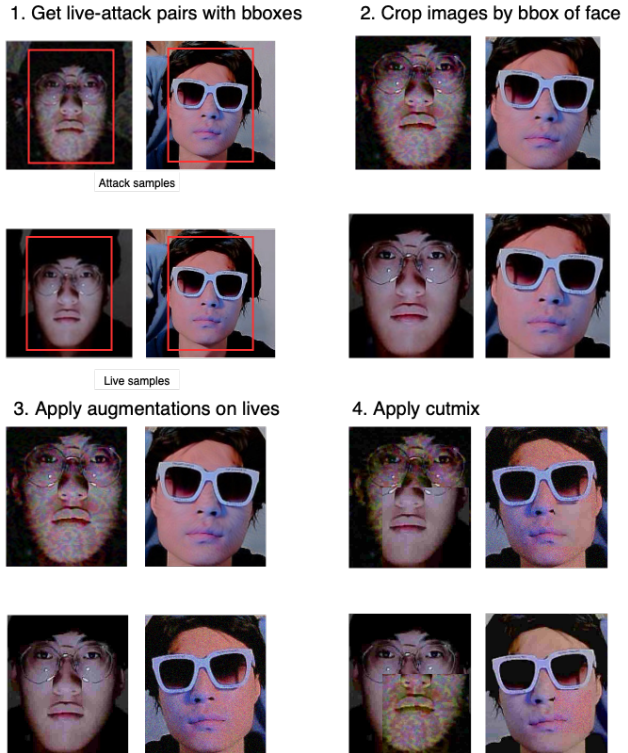


Figure 2. Overview of our data preprocessing steps used to obtain the final training pairs in our proposed pipeline: (1) Pairing attacks with corresponding lives. (2) Cropping image with bounding boxes. (3) Applying augmentations on live samples. (4) Applying CutMix augmentation strategy

stabilize training on a highly constrained set of live samples and increase attention to distinguishing such artifacts, we leverage paired-sampling of live and attack images within each training batch.

We utilize the previously obtained mapping between each attack sample and its most similar live counterpart in our proposed approach. First, we sample half of the batch with spoofing attack samples, and then we append the most similar live sample for each attack in the batch. The final set of training pairs consists of 7 918 pairs.

Let \mathcal{S} denote the set of spoofing attack samples and \mathcal{L} the set of live samples in the training dataset. If the cardinality of the spoofing subset is significantly greater than that of the live subset, i.e.,

$$|\mathcal{S}| \gg |\mathcal{L}|,$$

then the proposed pairing strategy can act as an implicit oversampling mechanism for the live subset. Since the most similar live sample is selected for each spoofing sample, live samples from the smaller cohort \mathcal{L} are more likely to be sampled repeatedly, thereby increasing their influence during training.

3.3. Contrastive training

To improve the discriminative power of the learned representation we optimise a dual-objective consisting of Focal loss [19], and a supervised contrastive SupCon loss [20]. Let \mathbf{x} denote an input image, $\mathbf{f}_\theta(\mathbf{x}) \in \mathbb{R}^d$ the backbone feature vector, and $\mathbf{z} = \text{proj}(\mathbf{f}_\theta(\mathbf{x})) \in \mathbb{S}^{d-1}$ its ℓ_2 -normalised projection on the unit sphere. For a mini-batch $\mathcal{B} = \{(\mathbf{z}_i, y_i)\}_{i=1}^N$ the SupCon term for an anchor i is:

$$\mathcal{L}_{\text{supcon}}^{(i)} = -\log \frac{\sum_{j \neq i} \mathbf{1}[y_j = y_i] \exp\left(\frac{\mathbf{z}_i^\top \mathbf{z}_j}{T}\right)}{\sum_{k \neq i} \exp\left(\frac{\mathbf{z}_i^\top \mathbf{z}_k}{T}\right)} \quad (1)$$

$$\mathcal{L}_{\text{supcon}} = \frac{1}{N} \sum_{i=1}^N \mathcal{L}_{\text{supcon}}^{(i)}, \quad (2)$$

where T is the temperature hyperparameter.

4. Experiments

4.1. Experimental Setting

Dataset and protocol. All experiments are conducted on the train and development pack released for The 6th Face Anti-Spoofing Challenge – Unified Physical-Digital Attack Detection@ICCV 2025 (FAS-ICCV 2025). The dataset contains **23 367 images**, only **839** images are bona fide, while the remaining **21 528** represent spoofed samples from nine diverse attack categories. These include both presentation attacks (print, replay, cutouts) and digital manipulations (attribute editing, face swap, video-driven synthesis, and both pixel- and semantic-level adversarial perturbations).

Data augmentation. To mitigate class imbalance and improve generalization, we apply an Albumentations-based augmentation pipeline during training:

- Geometric: horizontal flip,
- Photometric: brightness/contrast ($\pm 10\%$), hue/saturation (± 10), gamma (range 80–120),
- Compression: JPEG quality sampled from [40, 60].

Additionally, we apply CutMix augmentation with probability=0.3, and $\alpha=0.6$ to both live and attack samples, which encourages the model to localize spoof-specific artifacts and mitigates overfitting.

Network architecture. Our model backbone is **ConvNeXt-v2-Tiny** (28M parameters) [21], pretrained on ImageNet1K [22]. Each input face-cropped image is resized to $224 \times 224 \times 3$ (standard RGB), globally average-pooled by the backbone, and then passed to two heads:

1. a *binary classification head*, single fully-connected layer for live/attack prediction

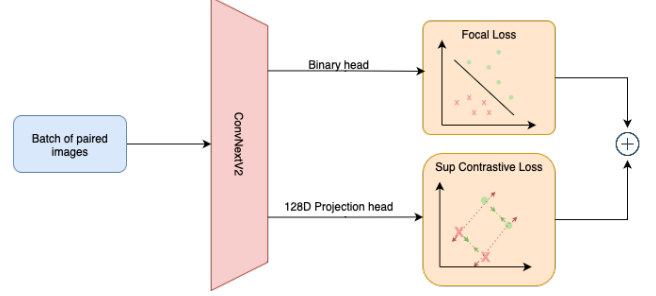


Figure 3. The proposed combination of loss functions used in our training strategy.

2. a *projection head*, two-layer MLP that produces 128-dimensional embeddings for contrastive training.

Loss function. Training minimizes a weighted sum of focal and supervised contrastive loss:

$$\mathcal{L} = \mathcal{L}_{\text{focal}} + \lambda \mathcal{L}_{\text{supcon}}$$

The training objective combines focal loss with a class-balancing factor $\alpha = 0.5$ and focusing parameter $\gamma = 0.7$ to counter label imbalance and a supervised contrastive loss evaluated over the entire mini-batch of identity-consistent live–attack pairs.

We use CutMix-augmented inputs and their mixed labels exclusively for the Focal loss head, while the SupCon head operates on original, unperturbed labels. This separation prevents the mixed-label targets produced by CutMix from corrupting the positive mask of the SupCon loss.

Evaluation metrics. The competition leaderboard is ranked by the **Average Classification Error Rate (ACER)** on the hidden test set. For completeness we additionally report

- **EER** – the Equal-Error Rate at the ROC operating point where FAR = FRR;
- **APCER** – overall Attack Presentation Classification Error Rate;
- **BPCER** – overall Bona-Fide Presentation Classification Error Rate;
- **ACER** – the mean of APCER and BPCER values;

The checkpoint with the lowest validation EER is selected for final submission.

The metrics are defined as:

$$\begin{aligned} \text{EER: } & \text{FAR} = \text{FRR}, \\ \text{ACER} &= \frac{\text{APCER} + \text{BPCER}}{2}, \\ \text{APCER} &= \frac{\text{FP}}{\text{FP} + \text{TN}}, \\ \text{BPCER} &= \frac{\text{FN}}{\text{FN} + \text{TP}}. \end{aligned}$$

Setup	ACER ↓	Acc ↑	AUC ↑
w Lives Augs & SupCon	0.0085	0.9831	0.9910
w/o SupCon	0.0177	0.9646	0.9871
w/o Lives Augmentations	0.0862	0.9046	0.9646

Table 2. Validation results under different training setups.

Training details. We fine-tuned the backbone on resized face crops. For data filtering, we used $\tau_{sim} = 0.9$ as cosine similarity threshold. Mini-batches of 32 images are processed on 2x NVIDIA L4 24GB GPU; each nominal epoch spans half of the training set, and the run lasts 20 epochs. Optimization employs *AdamW* with weight-decay 1.1×10^{-5} . A 5% warm-up cosine schedule anneals the rate from 1.82×10^{-4} to 6.8×10^{-7} in a single cycle. The objective combines binary focal loss ($\alpha = 0.5$, $\gamma = 0.7$) with supervised contrastive loss (projection dimension 128, temperature $\tau = 0.14$, weight $\lambda = 0.3$). CutMix applied to both live and attack crops with probability 0.3 and $\alpha = 0.6$. The checkpoint achieving the lowest validation EER was retained for submission.

4.2. Evaluation

We evaluated the Paired Liveness Contrastive Framework on the official validation split of "The 6th Face Anti-Spoofing: Unified Physical-Digital Attacks Detection@ICCV 2025". Experiments were conducted with and without key components: data pairing, asymmetric live-frame augmentation, and supervised contrastive learning, whose individual impacts on ACER reduction are detailed in Tab. 2. Our proposed approach demonstrated 2.10% ACER on the hidden test set of the challenge. Together, these results validate the effectiveness and practicality of our unified framework for simultaneous detection of both physical and digital face attacks.

4.3. Ablation Study

Data filtering threshold. To determine the optimal cosine similarity threshold τ_{sim} for pairing attack samples with their most similar live counterparts, we conducted a grid search over threshold values from 0.84 to 0.91. Lower thresholds admit more attack–live pairs into the training set, increasing dataset size but also allowing a higher proportion of loosely matched identities. Therefore, higher thresholds ensure stronger identity consistency between pairs, but overly restrictive filtering risks removing diverse training examples. As shown in Tab. 3, the threshold $\tau_{sim} = 0.90$ yielded the lowest ACER (1.08%) and the highest accuracy (97.85%) on the validation set. This indicates that stricter matching leads to more consistent identity pairs, enabling the model to focus on liveness-related cues. Based on these results, we adopted $\tau_{sim} = 0.90$ for our experiments.

Threshold	Dataset Size	ACER ↓	Acc ↑	AUC ↑
0.84	10339	0.1426	0.8686	0.9550
0.85	10131	0.0661	0.9446	0.9749
0.86	9887	0.0621	0.9527	0.9850
0.87	9637	0.0785	0.9199	0.9673
0.88	9362	0.0789	0.9192	0.9706
0.89	9036	0.0769	0.9231	0.9747
0.90	8669	0.0108	0.9785	0.9903
0.91	8207	0.0594	0.9581	0.9908

Table 3. Effect of cosine similarity threshold on validation performance in the paired-sampling filtering stage.

Hyperparameter Sensitivity Analysis. To assess the influence of key augmentation and contrastive learning parameters on validation performance, we conducted a grid search over the CutMix parameters α and p , as well as the supervised contrastive loss weight λ_{supcon} and temperature T . Fig. 5 visualizes the validation EER as a function of these hyperparameters.

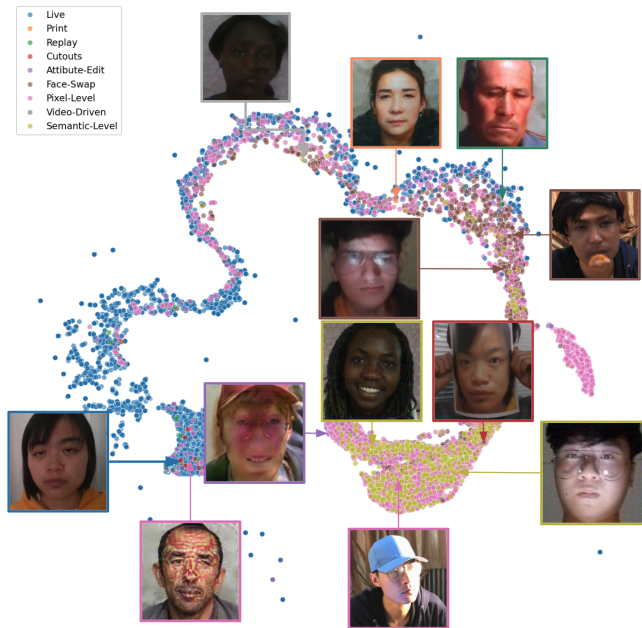
The top plot reveals that low to moderate CutMix probabilities $p \approx 0.15$ – 0.3 combined with $\alpha \approx 0.6$ – 1.0 tend to minimize EER, suggesting that excessive CutMix usage or overly aggressive blending may obscure liveness cues. On the bottom, the optimal supervised contrastive configuration is found near $\lambda_{supcon} \approx 0.2$ – 0.3 and $T \approx 0.15$ – 0.2 , balancing feature compactness for genuine samples with sufficient separation from attack embeddings. These results informed the final hyperparameter settings used in our challenge submission.

UMAP analysis. To better understand the distribution of live and attack samples, we conducted a UMAP analysis on the learned feature representations.

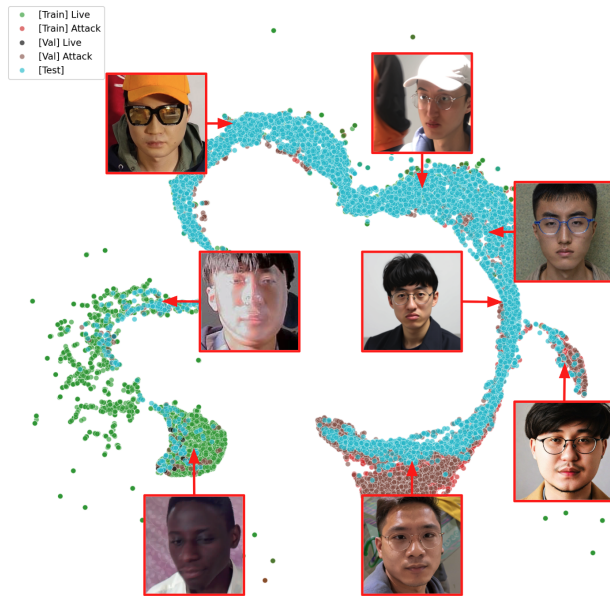
Fig. 4a presents a UMAP projection of various spoof types. Each point corresponds to a sample in the dataset, color-coded according to the type of manipulation.

We observe a clustering of live samples, which are separated from the majority of attack types. Additionally, certain spoof categories tend to form localized clusters, indicating that the model learns discriminative patterns not only between live and fake samples, but also among different kinds of attacks. This suggests that some attack types share similar visual or statistical characteristics in the learned feature space. Example images are overlaid to provide visual context for these clusters.

Fig. 4b shows a UMAP projection plot where the samples are grouped according to dataset split and label. We observe significant overlap between live samples from the training set and visually obvious attacks from the validation and test sets. This suggests that despite apparent differences from a human perception perspective, the learned representation sometimes struggles to draw clear boundaries, proba-



(a) Learned feature space for different classes



(b) UMAP projection grouped by dataset split.

Figure 4. UMAP projections used in the ablation study. Example images are shown to illustrate the types of attacks present in each cluster.

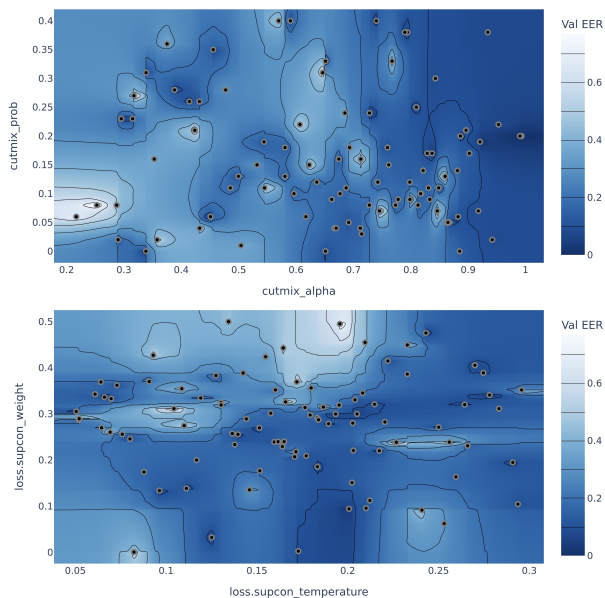


Figure 5. Impact of CutMix parameters (**top**) and supervised contrastive loss parameters (**bottom**) on validation EER. Darker regions indicate lower EER values. The CutMix plot varies α and probability p , while the SupCon plot varies loss weight λ_{supcon} and temperature T .

bly due to the limited variability in training data or the complexity of generalizing across different distributions. They

also highlight which spoof types may be more challenging for generalization in the proposed approach.

Model cues. On UniAttackData our model mostly attends to cues that are also obvious to a human observer. As shown in Fig. 6, (b) and (c) highlight specular reflections and texture inconsistencies on the glasses/skin, while (a) focuses on the mask boundary and local edge discontinuities.

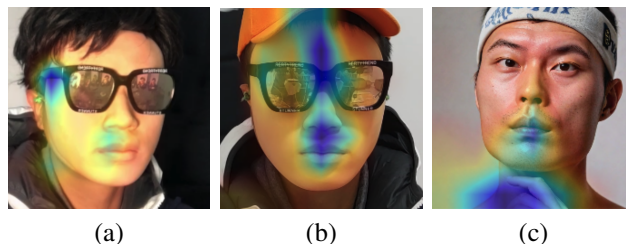


Figure 6. Model attention on attacks. The train detector focuses on human-visible cues: mask edge discontinuities (a), specular highlights (b), and skin texture anomalies (c)

5. Conclusion

In this paper, we presented a paired-sampled contrastive framework for face attack detection that jointly addresses both physical presentation attacks and digital forgeries within a single model. Our contrastive parallel training strategy leverages automatically paired live and spoof images, and trained via a combined focal and contrastive loss

in order to learn robust liveness representations. We implemented this approach using a lightweight ConvNeXt-v2-Tiny backbone with the CutMix technique, and achieved an ACER of 2.10% in "The 6th Face Anti-Spoofing: Unified Physical-Digital Attacks Detection@ICCV 2025" challenge, placing it among the top-performing methods.

Extensive experiments show that our method achieves high detection accuracy ACER of 2.10% on the challenge dataset, while maintaining low computational overhead (4.46 GFLOPs) suitable for real-time deployment. Moreover, our analysis highlights the benefit of contrastive learning and asymmetric augmentation in improving generalization to unseen attack types and domains.

We believe that a unified detection system, informed by both presentation and digital attack cues, will be critical for securing next-generation face recognition systems against evolving threats.

References

- [1] Haocheng Yuan, Ajian Liu, Junze Zheng, Jun Wan, Jiankang Deng, Sergio Escalera, Hugo Jair Escalante, Isabelle Guyon, and Zhen Lei. Unified physical-digital attack detection challenge. In *Proceedings of the IEEE/CVF Conference on Computer Vision and Pattern Recognition*, pages 919–929, 2024. 1, 2
- [2] Zitong Yu, Rizhao Cai, Zhi Li, Wenhan Yang, Jingang Shi, and Alex C Kot. Benchmarking joint face spoofing and forgery detection with visual and physiological cues. *IEEE Transactions on Dependable and Secure Computing*, 21(5): 4327–4342, 2024. 2
- [3] Mingxing Tan and Quoc Le. Efficientnet: Rethinking model scaling for convolutional neural networks. In *International conference on machine learning*, pages 6105–6114. PMLR, 2019. 2
- [4] Anjith George, Zohreh Mostaani, David Geissenbuhler, Olegs Nikisins, André Anjos, and Sébastien Marcel. Biometric face presentation attack detection with multi-channel convolutional neural network. *IEEE transactions on information forensics and security*, 15:42–55, 2019. 2
- [5] Alexey Dosovitskiy, Lucas Beyer, Alexander Kolesnikov, Dirk Weissenborn, Xiaohua Zhai, Thomas Unterthiner, Mostafa Dehghani, Matthias Minderer, Georg Heigold, Sylvain Gelly, et al. An image is worth 16x16 words: Transformers for image recognition at scale. *arXiv preprint arXiv:2010.11929*, 2020. 2
- [6] Anwei Luo, Rizhao Cai, Chenqi Kong, Yakun Ju, Xiangui Kang, Jiwu Huang, and Alex C Kot Life. Forgery-aware adaptive learning with vision transformer for generalized face forgery detection. *IEEE Transactions on Circuits and Systems for Video Technology*, 2024. 2
- [7] Van Dat Nguyen, Nesryne Mejri, Inder Pal Singh, Polina Kuleshova, Marcella Astrid, Anis Kacem, Enjie Ghorbel, and Djamilia Aouada. Laa-net: Localized artifact attention network for quality-agnostic and generalizable deepfake detection. In *Proceedings of the IEEE/CVF Conference on Computer Vision and Pattern Recognition (CVPR)*, pages 17395–17405, 2024. 2
- [8] Fabrizio Guillaro, Davide Cozzolino, Avneesh Sud, Nicholas Dufour, and Luisa Verdoliva. Trufor: Leveraging all-round clues for trustworthy image forgery detection and localization. In *Proceedings of the IEEE/CVF conference on computer vision and pattern recognition*, pages 20606–20615, 2023. 2
- [9] Shichao Dong, Jin Wang, Renhe Ji, Jiajun Liang, Haoqiang Fan, and Zheng Ge. Implicit identity leakage: The stumbling block to improving deepfake detection generalization. In *Proceedings of the IEEE/CVF Conference on Computer Vision and Pattern Recognition*, pages 3994–4004, 2023. 2
- [10] Kaede Shiohara and Toshihiko Yamasaki. Detecting deepfakes with self-blended images. In *Proceedings of the IEEE/CVF conference on computer vision and pattern recognition*, pages 18720–18729, 2022. 2
- [11] Baojin Huang, Zhongyuan Wang, Jifan Yang, Jiabin Ai, Qin Zou, Qian Wang, and Dengpan Ye. Implicit identity driven deepfake face swapping detection. In *Proceedings of the IEEE/CVF conference on computer vision and pattern recognition*, pages 4490–4499, 2023. 2
- [12] Andreas Rossler, Davide Cozzolino, Luisa Verdoliva, Christian Riess, Justus Thies, and Matthias Nießner. Faceforensics++: Learning to detect manipulated facial images. In *Proceedings of the IEEE/CVF international conference on computer vision*, pages 1–11, 2019. 2
- [13] Yuezun Li, Xin Yang, Pu Sun, Honggang Qi, and Siwei Lyu. Celeb-df: A large-scale challenging dataset for deepfake forensics. In *Proceedings of the IEEE/CVF conference on computer vision and pattern recognition*, pages 3207–3216, 2020.
- [14] Brian Dolhansky, Joanna Bitton, Ben Pflaum, Jikuo Lu, Russ Howes, Menglin Wang, and Cristian Canton Ferrer. The deepfake detection challenge (dfdc) dataset. *arXiv preprint arXiv:2006.07397*, 2020. 2
- [15] Bojia Zi, Minghao Chang, Jingjing Chen, Xingjun Ma, and Yu-Gang Jiang. Wilddeepfake: A challenging real-world dataset for deepfake detection. In *Proceedings of the 28th ACM international conference on multimedia*, pages 2382–2390, 2020. 2
- [16] Debayan Deb, Xiaoming Liu, and Anil K Jain. Unified detection of digital and physical face attacks. In *2023 IEEE 17th International Conference on Automatic Face and Gesture Recognition (FG)*, pages 1–8. IEEE, 2023. 2
- [17] Christian Szegedy, Sergey Ioffe, Vincent Vanhoucke, and Alexander A. Alemi. Inception-v4, inception-resnet and the impact of residual connections on learning. In *Proceedings of the 31st AAAI Conference on Artificial Intelligence*, pages 4278–4284, 2017. URL <https://arxiv.org/abs/1602.07261>. 3
- [18] Kaipeng Zhang, Zhanpeng Zhang, Zhifeng Li, and Yu Qiao. Joint face detection and alignment using multi-task cascaded convolutional networks. *IEEE Signal Processing Letters*, 23(10):1499–1503, 2016. doi: 10.1109/LSP.2016.2603342. URL <https://arxiv.org/abs/1604.02878>. 3
- [19] Tsung-Yi Lin, Priya Goyal, Ross Girshick, Kaiming He, and Piotr Dollár. Focal loss for dense object detection. In *Pro-*

ceedings of the IEEE international conference on computer vision, pages 2980–2988, 2017. 4

- [20] Prannay Khosla, Piotr Teterwak, Chen Wang, Aaron Sarna, Yonglong Tian, Phillip Isola, Aaron Maschinot, Ce Liu, and Dilip Krishnan. Supervised contrastive learning. In *Advances in Neural Information Processing Systems*, volume 33, pages 18661–18673, 2020. URL <https://arxiv.org/abs/2004.11362>. 4
- [21] Sanghyun Woo, Shoubhik Debnath, Ronghang Hu, Xinlei Chen, Zhuang Liu, In So Kweon, and Saining Xie. Convnext v2: Co-designing and scaling convnets with masked autoencoders. In *2023 IEEE/CVF Conference on Computer Vision and Pattern Recognition (CVPR)*, pages 16133–16142, 2023. doi: 10.1109/CVPR52729.2023.01548. 4
- [22] Jia Deng, Wei Dong, Richard Socher, Li-Jia Li, Kai Li, and Li Fei-Fei. Imagenet: A large-scale hierarchical image database. In *Proceedings of the IEEE Conference on Computer Vision and Pattern Recognition (CVPR)*, pages 248–255, 2009. doi: 10.1109/CVPR.2009.5206848. URL https://image-net.org/static_files/papers/imagenet_cvpr09.pdf. 4